Integration of Pump-Storage Batteries in Offshore Wind Farms

Integration of Pump-Storage Batteries in Offshore Wind Farms: Evaluation of Effects on Power Exchange

Emilija Lazdanaite[1], Phuong Nguyen[1], Minh-Quan Tran[1], Frits Bliek[2], Marijn van Rooij[2]
[1]Electrical Energy Systems Group, Eindhoven University of Technology (TU/e)
[2]Ocean Grazer B.v
Email: p.nguyen.hong@tue.nl

2022 IEEE PES Innovative Smart Grid Technologies - Asia (ISGT Asia) | 979-8-3503-9966-0/22/$31.00 ©2022 IEEE | DOI: 10.1109/ISGTASIA54193.2022.10003552

***Abstract*—While having a significant contribution to the total installed capacity, rapid development of offshore wind farms (OWFs) pose technical challenges for supply-demand balancing and onshore grid capacity. Various storage technologies are being considered to integrate in OWFs to combat these issues in the local offshore grid. This paper introduces a unique concept of pump-storage batteries which can enhance demand and supply management of the OWF and improve grid utilization. This paper will present specifications of this proposed battery model, technology used for control of pump-turbine applications, and presents the simulation set-ups and results for week-long operation of the battery.**

***Index Terms*—Offshore wind farms, power exchange, pump-storage batteries.**

I. Introduction

The recent International Panel on Climate Change report [1] highlights the urgent need to move away from fossil fuels to renewable energy sources (RES). Offshore wind is set to play a big role in this energy transition – the European Commission has set a target of 300 GW offshore wind capacity for 2050 [2]. The government of the Netherlands alone is aiming for 27% – or 11 GW – of its energy to come from RES by 2030 [3]. This rapid development is however posing challenges for supply-demand balancing due to the stochastic generation of wind as well as expanding onshore grid capacity to accommodate such large-scale renewable energy sources (RES).

Battery systems are being deployed to combat these issues in the local offshore grid. In [4] authors propose to use battery energy storage systems (BESS) to help mitigate reactive power control in multi-terminal HVDC systems. In [5], liquid metal battery storage is used for energy arbitrage: time-shifting the renewable energy to discharge at higher-priced hours. However, lithium-ion batteries are expensive for long life-times, while liquid metal batteries are quite new and have not yet been deployed to the best of the authors knowledge. The aforementioned North Sea Power Hub is planning to store energy by converting it to hydrogen using electrolysis. However, the technology to do this is still in developmental stages. A detailed list and categorization of electrical energy storage (EES) systems can be found in [6].

Large-scale pumped-hydro energy storage (PHES) is a mature technology that has been used in tandem with RES to provide load-balancing because of its rapid ramp-up capabilities, reliability and short life cycle costs compared to its battery energy storage alternatives [7], [8]. 99% of worldwide storage capacity is made up of PHES, however, large PHES is constrained by site selection, and therefore suffers from long construction time and high capital investment [9].

Small-scale PHES such as one invented by Ocean Grazer is an alternative concept which is distributed locally in the offshore wind farm. It is positioned under water, on the ocean floor, and consists of two reservoirs: a rigid concrete reservoir under the earth, and a flexible reservoir on the ocean floor. The flexible reservoir is under high pressure from the surrounding ocean water (see Fig. 1(b)). These two reservoirs are linked with five sets of motor-generator machines coupled to pump-turbines. When the battery is fully charged, the flexible reservoir is filled with water and has high potential energy caused by the surrounding ocean water. When power needs to be discharged, water flows from this flexible reservoir through the hydro-turbines into the concrete reservoir. When power needs to be stored, water is pumped by the five sets of of machines to the flexible reservoir.

This paper aims to investigate the potential uses of a locally dispatched PHES and its performance. Considering the previous discussion, the interesting use-cases are:

1) **Demand and supply management**: This will be done by the battery compensating the difference between active power generated by the wind turbines and the forecast.
2) **Cable utilization improvement**: Peak shaving will be employed to level out power transmission through cable to shore.

This paper discusses the Ocean Battery model, technology used for control of pump-turbine applications, and presents the simulation set-ups and results for week-long operation of the battery.

II. Ocean Battery model

As mentioned previously in Section I, the Ocean Battery consists of five units made up of pump-turbines coupled to motor-generators. They share a piping system and the closed-loop reservoirs. Closed-loop pump-storage systems do not have natural inflow or outflow of water, and therefore have

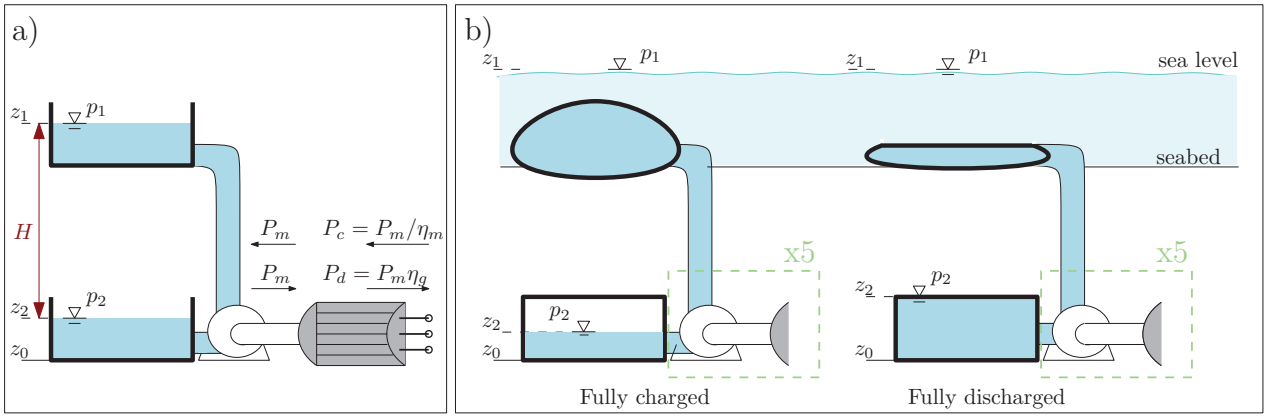

Fig. 1: Illustrations: a) open-loop or large closed loop hydroturbine configuration b) closed-loop small-scale Ocean Battery in fully charged and fully discharged modes. The Ocean Battery has one flexible reservoir, one rigid reservoir, and 5 sets of pump-turbine coupled with motor-generator.

limited charge/discharge capacity and operational time. The reservoirs of the Ocean Battery contain water that is separate from the sea water. This chapter discusses the functionality and important parameters of the two main machines making up the five units – the pump-turbine and the motor-generator.

A. Pump-turbine

The mechanical power extracted from the water by the pump-turbine is [10]

$$P_m = \eta_h \rho g \dot{V} H \quad [\text{W}] \tag{1}$$

and mechanical power used to put energy into the water by the pump-turbine is

$$P_m = \frac{\rho g \dot{V} H}{\eta_\text{p}} \quad [\text{W}] \tag{2}$$

The energy storage capacity can be calculated at the fully charged point, where the head is at it's maximum [11]:

$$E_\text{storage} = \frac{\rho g H_\text{max} V_\text{res}}{3.6 \cdot 10^9} \quad [\text{MWh}] \tag{3}$$

where V_res is the upper reservoir volume, and division by $3.6 \cdot 10^9$ converts from joules [J] to megawatt-hours [MWh].

For power output and energy storage capacity, the volume flow rate $\dot{V}$ [m^3/s] and the head H [m] are two important variables for a pump-turbine, and are influenced by the physical construction of the fluid system. The head is a measure of the potential energy stored, and is related to the height difference and potential difference between the water levels of the two reservoirs. In an open-loop pump-storage system such as in Fig. 1(a), these levels are constant, because of the natural inflow and outflow of water. The physical construction of the Ocean Battery as in Fig. 1(b) leads to a varying head between charging and discharging, as the level of water in the rigid reservoir varies, while the level of the flexible reservoir can be taken as the sea level, which remains constant.

An important variable for the battery as a whole is the state of chare (SOC), indicating the current charge of the battery. At a given point in time t it can be defined as:

$$\text{SOC}_t = \text{SOC}_{t-\Delta t} + \frac{\dot{V}_{\text{res},t}}{V_\text{total}} \Delta t \cdot 100 \quad [\%] \tag{4}$$

The total volume flow rate of water coming into the flexible reservoir is the accumulation of flow rates of all five turbomachines:

$$\dot{V}_\text{total} = \sum_{i=1}^{5} \dot{V}_{\text{in},i} - \sum_{i=1}^{5} \dot{V}_{\text{out},i} \quad [\text{m}^3/\text{s}] \tag{5}$$

where i denotes the hydro-turbine set, $\dot{V}_\text{in}$ is the rate of water flowing into the flexible reservoir (charging), and $\dot{V}_\text{out}$ is the rate of water flowing out of the flexible reservoir (discharging).

B. Electrical Machines

Both PHES and wind generation use electrical machines. In the former, the prime mover is the pump-turbine, in the latter it is a wind turbine. The basic principal of an electrical machine is electromagnetic fields interacting between rotor (rotating part) and stator (stationary part) of the machine.

The apparent power consumed or generated by one phase of an AC electrical machine can be described by the equation [12]

$$\mathbf{S} = \mathbf{V}\mathbf{I}^* = P + jQ \quad [\text{VA}] \tag{6}$$

where $\mathbf{V}$ is the complex phase voltage (line-to-neutral), $\mathbf{I}^*$ is the complex conjugate of the phase current. P is the real (active) power [W] and represents the useful work being performed. Q is the reactive power [VAr], which represents the energy transfers related to capacitive components in a circuit [13], [14]. These transfers result in energy loss in transmission lines, as well as node voltage changes.

The magnitude and phase of the apparent power are given as

$$|S| = \sqrt{P^2 + Q^2}$$
$$\theta = \tan\left(\frac{Q}{P}\right). \tag{7}$$

An important parameter is the power factor, defined as:

$$\text{PF} = \cos(\theta). \tag{8}$$

In the simplest terms, the power factor shows how much useful power (active power P) is being produced or consumed in relation to the apparent power S.

C. Variable Speed

The current trend for PHES is to move towards variable speed drives. Most variable-speed pumped-hydro and pump-storage systems use one of two machine configurations: the pump-turbine coupled to a DFIM or PMSM, both of which are coupled to the grid via a back-to-back converter. It was found that in large scale PHES, 83.4% use DFIM because it only needs a partial rated converter to drive the rotor. 55% of micro or pico hydro-electric plants use PMSM because of its efficiency and high grid fault tolerance (robustness). The other 45% use DFIM. A comprehensive review of different types of converters and controls used for PHES is given in [8].

D. Back-to-back Converter

The back-to-back converters are made up of two voltage source (VSC) converters: a machine side converter (MSC) and a grid-side converter (GSC). These are usually 2-level (each phase is controlled by two switches, usually insulated-gate bipolar transistors (IGBTs) with parallel diodes allowing for bi-directional power flow). Multi-level VSCs can also be found in large-scale PHES [8] because less voltage stress is exerted on the switches than when using 2-level converters. The switches are controlled by a pulse-width modulated (PWM) signal. This causes harmonics, however they are of high frequency and usually can be easily filtered out. This PWM signal controls the phase of field current, and therefore according to (6) control the reactive power output.

III. Simulations and Results

A. Simulation Set-up

The simulations were carried out in DIgSILENT PowerFactory 2021, using Python 3.9 using Quasi-Dynamic analysis. An offshore wind farm connected to onshore grid through a HVDC link as seen in Fig. 2. This offshore wind farm consists of 80 wind turbines with 5 MW power rating, connected to an 0.69 kV bus. Each wind turbine is equipped with an Ocean Battery, which is made up of five electrical machines rated at 200 kW with a terminal voltage of 400 V. The Ocean Battery then has the power capacity of 1 MW in charging mode, and 0.77 MW in discharging mode according to:

$$P_{\text{max,c}} = \frac{P_m}{\eta_m} = \frac{\rho g H_{\max} \eta_{\text{water}}}{\eta_p \eta_m}$$
$$P_{\text{max,d}} = P_m \eta_g = \rho g H_{\max} \eta_{\text{water}} \eta_p \eta_m \tag{9}$$

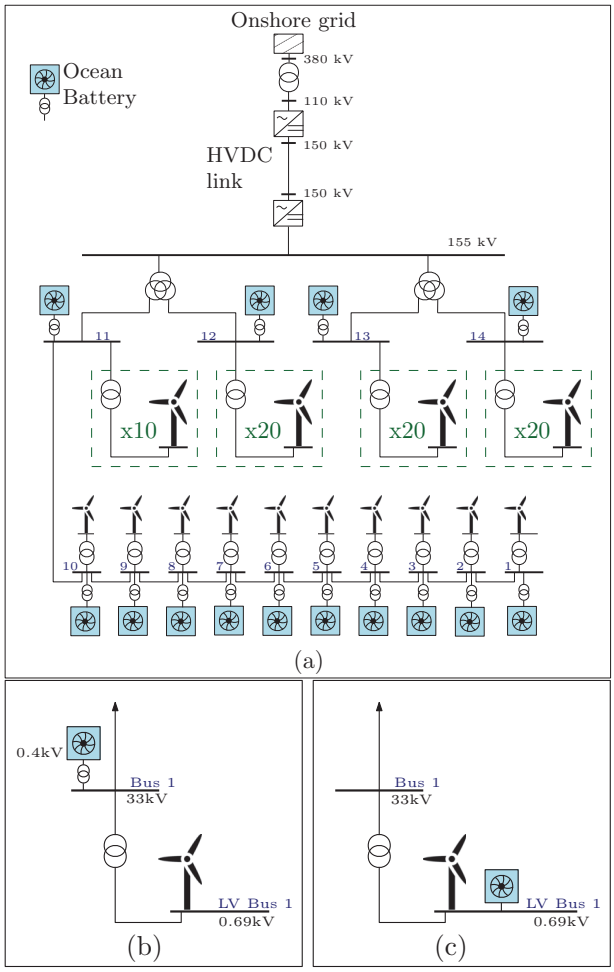

Fig. 2: Grid used for simulations. The AC onshore grid is connected to the AC offshore wind turbines by an HVDC link. Each wind turbine is equipped with an Ocean Battery.

where the head loss due to friction of water in the piping is represented as the water run efficiency η_{water}. The volume flow rate at any given time step is then adjusted proportionally to the output power as:

$$\dot{V}_{\text{in}} = \frac{P_o}{P_{\text{max,c}}}$$
$$\dot{V}_{\text{out}} = \frac{P_o}{P_{\text{max,d}}}. \tag{10}$$

The electrical machines in the Ocean Battery are chosen to be static generator elements: a simple PQ bus which can behave as either a DFIM or a PMSM with converter. It can be programmed to output P and Q values set by the user, therefore it is easy to control. Additionally, transients and dynamic operation can be excluded with quasi-dynamic simulation, as the data has a 15 minutes time step.

The cavitation and stability limits are ignored in these results, as the appropriate machines for the units have not been

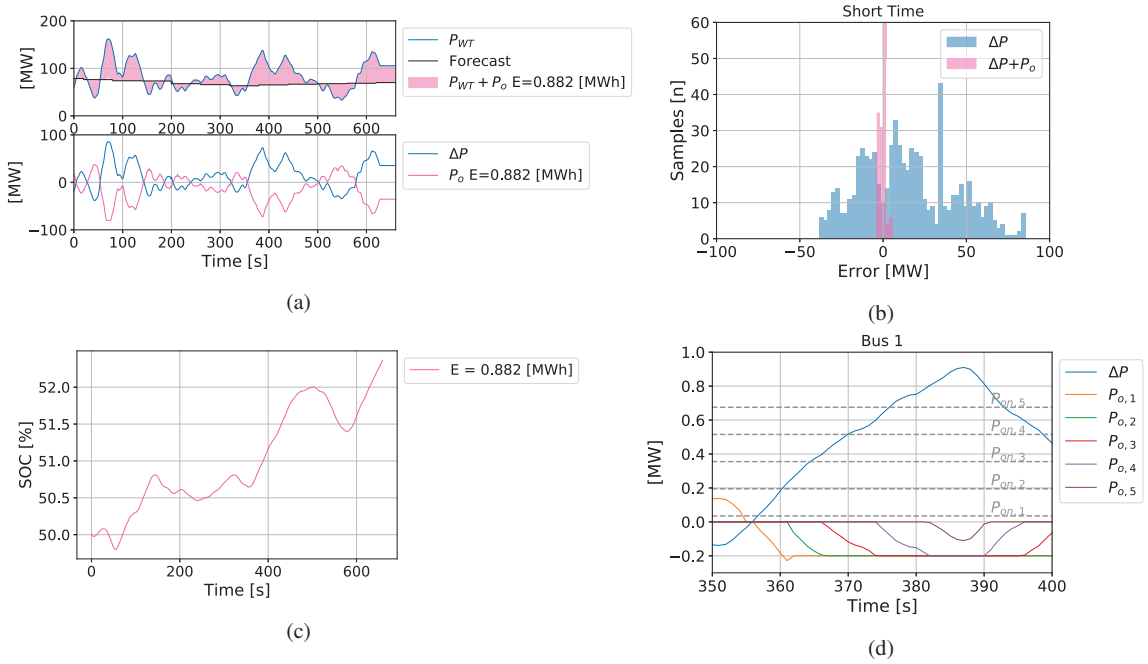

Fig. 3: Active power compensation for 11 minutes: (a) time-domain characteristics of generated power P_{WT}, expected power *Forecast*, the difference between them ΔP and the output of the combined Ocean Batteries P_o for storage capacity $E = 0.882$ [MWh] (b) Histogram of errors between expected and generated power, without the battery ΔP and with $\Delta P + P_o$ (c) SOC of the battery, climbing with time as mostly overproduction occurs (d) zoom-in of power output $P_{o,i}$ of each electrical machine in one Ocean Battery.

chosen yet, and therefore these limits are difficult to estimate accurately. The generation and forecast data is retrieved from Growind, a 63 MW wind farm consisting of 21 wind turbines. This data is adjusted to correspond to the 5 MW rating of the wind turbines. As per the Introduction, three applications of the Ocean Battery are investigated, which are discussed in the following subsections.

B. Demand and Supply Management

The set-up is as in Fig. 2 (a), with the Ocean Battery being connected to the 33 kV bus of the wind turbine through a 400V/33kV transformer rated at 1.2 MVA as in Fig. 2 (b). Each Ocean Battery is controlled to generate or absorb the power difference ΔP between the active power being generated by the wind turbine and the forecasted active power:

$$\begin{aligned} \Delta P &= P_{\text{WT}} - \textit{Forecast} \\ P_o &= \sum_{i=1}^{5} P_{o,i} \end{aligned} \tag{11}$$

where P_o is the output of one battery, while $P_{o,i}$ is the individual power output of the five machines in a battery, see Fig.3(d).

In previous research on the Ocean Battery it was shown through a techno-economic analysis that for a 700 MW wind farm:

$$\begin{aligned} E_{\text{cap}} &= 133.5 \quad [\text{MWh}] \\ P_{\text{cap}} &= 267.3 \quad [\text{MW}] \end{aligned} \tag{12}$$

where E_{cap} and P_{cap} are respectively the energy capacity and power capacity of the deployed storage. This means that for every megawatt produced by the wind farm, the Ocean Battery storage facilities have to have a power capacity of 0.3814 MW with about 0.19 MWh. For a 5 MW wind turbine, this would amount $E_{\text{storage}} = 0.96$ MWh. From (3), the storage capacity reflects either the water volume stored in the battery, or the head and volume flow rate. For a given output P in (1):

$$\begin{aligned} \frac{H}{\dot{V}} &\propto P \\ \frac{H}{\dot{V}} &\propto E \\ V_{\text{res}} &\propto E. \end{aligned} \tag{13}$$

Because of the closed-loop nature of the Ocean Battery, the bigger the storage capacity, the longer the battery can operate. Different storage capacities have been investigated, starting with a storage capacity of $E = 0.882$ [MWh], which corresponds to an hour of constant charge/discharge at the nominal volume flow rate $\dot{V}$.

Fig. 3 shows results of power compensation for a time-span of 11 minutes: it shows that for this short time, the Ocean

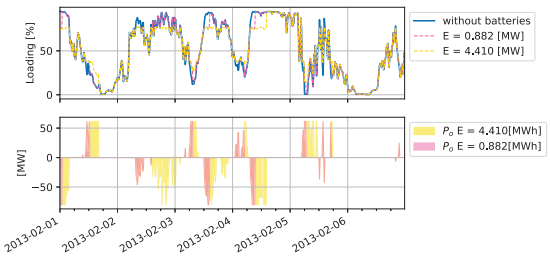

(a)

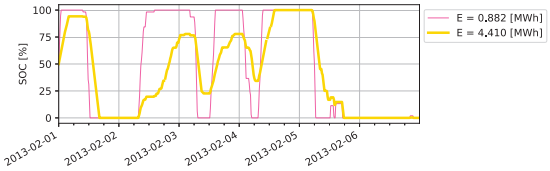

(b)

Fig. 4: HVDC cable loading results with increasing E. (a) time-domain characteristics of cable loading (%) and cumulative power outputs of the batteries (b) the SOC for two E values over time

Battery manages to track and compensate for the active power difference(Fig. 3 (a)) and the error ΔP is minimized (Fig. 3 (b)). The SOC in Fig. 3 (c) is climbing with time, as mostly overproduction occurs. The power output of each electrical machine is illustrated in Fig. 3 with the measured values at which the machine turns to $P_{\text{on,i}}$.

C. Cable Utilization Improvement

The set-up is as in the previous application, but now the goal is to bring down the loading of the DC line. This is done by the output of the Ocean Battery charging as the wind turbine power output reaches 4 MW, and discharges when the wind turbine goes below 2 MW. The error ΔP that is being compensated for is

$$\Delta P = P_{\text{WT}} \quad \text{for } P_{\text{WT}} \geq 4[\text{MW}] \text{ or} P_{\text{WT}} \leq 2[\text{MW}]. \tag{14}$$

Fig. 4 shows results of cable loading compensation. A similar problem is observed as in the previous section – the Ocean Battery produces active power only if it has not reached the limits of SOC.

IV. Conclusion

This paper presents a quasi-dynamic model of the Ocean Battery. It outlines the challenges of offshore wind and the need for battery storage, then gives a summary of technologies used in PHES, discusses how the dynamic behaviour of pump-turbines influences the power output and control of the electrical machine. The influence of physical construction of the Ocean Battery on the capabilities of active and reactive power consumption are presented through simulations of three use cases. When controlling the active power of the battery to compensate the difference between wind generation and forecast, a smaller error is reached when the capacity of the battery is increased, but this does not correspond to high magnitude error elimination. This means that the battery is not necessarily reliable for long-term operation unless it has a large enough storage capacity, or the battery dispatch is controlled with SOC tracking. When controlling to compensate for peaks of generated power, the battery can work continuously for longer periods of time without reaching SOC limits. However, it is shown that it is important to discharge the battery by an appropriate amount before encountering a peak, so SOC limits are not reached during a power peak. This can be mitigated by storage increase or coordination of battery sets.

V. Acknowledgments

The work leading to this paper is partially funded by H2020 project FlexiGrid, FAIR-PLAY and TROEF project from TKI Urban Energy and RVO, the Netherlands.

References

[1] V. Masson-Delmotte, P. Zhai, A. Pirani, S. L. Connors, C. Péan, S. Berger, N. Caud, Y. Chen, L. Goldfarb, M. I. Gomis, M. Huang, K. Leitzell, E. Lonnoy, J. Matthews, T. K. Maycock, T. Waterfield, O. Yelekçi, R. Yu, and B. Z. (eds.), "Climate change 2021: The physical science basis. contribution of working group i to the sixth assessment report of the intergovernmental panel on climate change," 2021. [Online]. Available: https://www.ipcc.ch/report/ar6/wg1/

[2] E. Commission, "Boosting offshore renewable energy for a climate neutral europe," 2020. [Online]. Available: https://ec.europa.eu/commission/presscorner/detail/en/ip_20_2096

[3] E. Wiebes, "Letter to parliament offshore wind energy roadmap 2030," 2018. [Online]. Available: https://www.government.nl/topics/renewable-energy/documents/parliamentary-documents/2018/03/27/letter-to-parliament-offshore-wind-energy-roadmap-2030

[4] H. Kim and M. Kim, "Optimal generation rescheduling for meshed ac/his grids with multi-terminal voltage source converter high voltage direct current and battery energy storage system," *Energy*, vol. 119, pp. 309–321, 2017. [Online]. Available: https://www.sciencedirect.com/science/article/pii/S0360544216317637

[5] J. Simpson, G. Hanrahan, E. Loth, G. Koenig, and D. Sadoway, "Liquid metal battery storage in an offshore wind turbine: Concept and economic analysis," *Renewable and Sustainable Energy Reviews*, vol. 149, p. 111387, 2021. [Online]. Available: https://www.sciencedirect.com/science/article/pii/S1364032121006729

[6] H. L. Ferreira, R. Garde, G. Fulli, W. Kling, and J. P. Lopes, "Characterisation of electrical energy storage technologies," *Energy*, vol. 53, pp. 288–298, 2013. [Online]. Available: https://www.sciencedirect.com/science/article/pii/S0360544213001515

[7] W. Yang and J. Yang, "Advantage of variable-speed pumped storage plants for mitigating wind power variations: Integrated modelling and performance assessment," *Applied Energy*, vol. 237, pp. 720–732, 2019. [Online]. Available: https://www.sciencedirect.com/science/article/pii/S0306261918319019

[8] K. R. Vasudevan, V. K. Ramachandaramurthy, G. Venugopal, J. Ekanayake, and S. Tiong, "Variable speed pumped hydro storage: A review of converters, controls and energy management strategies," *Renewable and Sustainable Energy Reviews*, vol. 135, p. 110156, 2021. [Online]. Available: https://www.sciencedirect.com/science/article/pii/S1364032120304470

[9] X. Luo, J. Wang, M. Dooner, and J. Clarke, "Overview of current development in electrical energy storage technologies and the application potential in power system operation," *Applied Energy*, vol. 137, pp. 511–536, 2015. [Online]. Available: https://www.sciencedirect.com/science/article/pii/S0306261914010290

[10] Y. A. Cengel and J. M. Cimbala, *Fluid Mechanics: Fundamentals and Applications. Fourth Edition in SI Units*, 2020.

[11] D. Stolten and V. Scherer, *Transition to Renewable Energy Systems*, 2013.

[12] M. E. El-Hawary, *Electrical Energy Systems*, 2000.

[13] N. Mohan, *Electric Power Systems: A First Course*, 2012.

[14] D. I. Leon Freris, *Renewable Energy in Power Systems*, 2008.